International Journal of Pharmacology

ISSN 1811-7775

science alert

ansinet
Asian Network for Scientific Information

OPEN ACCESS International Journal of Pharmacology

ISSN 1811-7775
DOI: 10.3923/ijp.2020.422.429

Research Article
Development and Evaluation of Febuxostat Loaded D-α-tocopheryl Polyethylene Glycol 1000 Succinate Micelles for Lung Cancer

[1]Mohammad Y. Alfaifi, [1]Ali A. Shati, [1,2]Serag Eldin I. Elbehairi, [3,4]Usama A. Fahmy, [3,4]Nabil A. Alhakamy and [3,4]Shadab Md.

[1]Department of Biology, Faculty of Science, King Khalid University, Abha 9004, Saudi Arabia
[2]Cell Culture Laboratory, Egyptian Organization for Biological Products and Vaccines (VACSERA Holding Company, 51 Wezaret El-Zeraa Street, Agouza, Giza, Egypt
[3]Department of Pharmaceutics, Faculty of Pharmacy, King Abdulaziz University, Jeddah, Saudi Arabia
[4]Center of Excellence for Drug Research and Pharmaceutical Industries, King Abdulaziz University, Jeddah, Saudi Arabia

Abstract

Background and Objective: Febuxostat (FBX) is a proven prophylactic agent in the management of tumor lysis syndrome in patients with malignant tumors. The clinical application of FBX is hindered due to poor solubility and bioavailability. The purpose of the present study was to develop miceller delivery of FBX using an amphiphilic and non-ionic macromolecule, D-α-tocopheryl polyethylene glycol 1000 succinate (TPGS) for the treatment of lung cancer. **Materials and Methods:** FBX-loaded TPGS micelles (TPGS-FBX-M) were formulated by thin-film hydration method and are characterized for particle size and morphology using dynamic light scattering techniques and transmission electron microscopy. Developed miceller formulation of FBX (TPGS-FBX-M) was further evaluated for entrapment efficiency and *in vitro* release. **Results:** Nano-sized spherical miceller deliveries of TPGS-FBX-M displayed a release of 72.7% within 12 h. The formulation was employed to assess cytotoxicity in adenocarcinomic human alveolar basal epithelial cells (A549), where TPGS-FBX-M micelles were found to reduce IC50 values as compared to free FBX which might be due to increased uptake of FBX and effectiveness against A549 cells. An increased cell cycle blockade at the G2/M phase improved apoptotic activity and a significant increase in the expression of caspase 3 for TPGS-FBX-M as compared to free FBX incubation *in vitro*. **Conclusion:** This impressive drug delivery platform for lipophilic agents can also be used to deliver other hydrophobic chemotherapeutics to target cancer cells for improves efficacy and safety.

Key words: Apoptosis, cell cycle, encapsulation efficiency, Febuxostat, lung cancer, micelles, nanotechnology

Citation: Mohammad Y. Alfaifi, Ali A. Shati, Serag Eldin I. Elbehairi, Usama A. Fahmy, Nabil A. Alhakamy and Shadab Md., 2020. Development and evaluation of febuxostat loaded D-α-tocopheryl polyethylene glycol 1000 succinate micelles for lung cancer. Int. J. Pharmacol., 16: 422-429.

Corresponding Author: Shadab Md., Department of Pharmaceutics, Faculty of Pharmacy, King Abdulaziz University, Jeddah, 21589, Saudi Arabia
Mohammad Y. Alfaifi, Department of Biology, Faculty of science, King Khalid University, Abha 9004, Saudi Arabia

Copyright: © 2020 Mohammad Y. Alfaifi *et al.* This is an open access article distributed under the terms of the creative commons attribution License, which permits unrestricted use, distribution and reproduction in any medium, provided the original author and source are credited.

Competing Interest: The authors have declared that no competing interest exists.

Data Availability: All relevant data are within the paper and its supporting information files.

INTRODUCTION

Lung cancer, a global health burden, is a leading cause of death among men and women. According to world estimates, 1.8 million new cases of lung cancer and 1.6 mortalities are recorded annually[1]. A poor rate of 5-year survival (17.8%) is common with lung cancer because of delayed diagnosis and inefficient treatment[2]. The common type of lung cancer, non-small cell lung cancer (NSCLC), is diagnosed among 80-85% of lung cancer patients, whereas rest are diagnosed with SCLC and lung carcinoid tumors[1]. Conventional treatment of lung cancer is still limited to surgical removal, radiation and chemotherapeutic applications, or combinations thereof; however, these treatments are found to be nonspecific and aggressive. Further, these nonspecific natures of treatments are frequently accompanied by unwanted severe toxicities to the healthy cells and tissues within the body[3]. Limitation of water solubility of hydrophobic therapeutics is a big hurdle in cancer chemotherapy, which urges formulation development under the umbrella of a novel drug delivery system[4]. Recent research on cancer therapy has gained remarkable interest in nanotechnology-based delivery, which could be predictable by the approval of several nanocarriers by the regulatory authorities in the improvement of safe and effective cancer treatment and hundreds of nanocarriers in the clinical stage, waiting for the safety results to reach to the bedside of the patients[5]. Among the nanocarriers, the amphiphilic spherical nanocarriers have gained much attention for the delivery of chemotherapeutics[6]. The dynamic structure of the micelles allows them to incorporate poorly soluble hydrophobic agents within the hydrophobic miceller core, whereas the outer hydrophilic shell stabilizes the delivery in an aqueous environment[7]. Due to their unique structure, it achieves greater kinetic and thermodynamic stability, whereas it can easily escape the reticuloendothelial system within the circulation because of the nanometric size range (<200 nm) and hydrophilic shell structure, leading towards improved enhanced permeability and retention effect (EPR effect)[8]. Use of amphiphilic copolymer, D-α-tocopheryl polyethylene glycol 1000 succinate (TPGS), a polyethylene glycol (PEG) conjugated natural vitamin E, found to gain interest in developing pharmaceutical formulations[5,9,10]. This amphiphilic, non-ionic macromolecule is found to be safe and efficient for the preparation of pharmaceutical micelles[11]. TPGS is widely used in the preparation of several nanocarriers[12-14] including micelle[11]. The presence of PEG in the miceller delivery found to improve the EPR effect further to prolong the circulation of nanocarrier, thus enhance bioavailability[15].

Here in this research we developed TPGS micelles for the delivery of febuxostat (FBX) to target lung cancer. FBX, a potent non-purine xanthine oxidase inhibitor, is a potential agent in the control of serum uric acid in gouty arthritis[16]. FBX is a proven prophylactic agent in the management of tumor lysis syndrome in patients with malignant tumors[17]. Here, we tried to establish FBX as an effective antitumor agent against lung cancer. The purpose of the present study was to develop miceller delivery of FBX using TPGS. The TPGS-FBX micelles were characterized and evaluated for their size, surface morphology, encapsulation efficiency and in vitro release pattern. Further, the FBX loaded micelles were tested for cytotoxicity and apoptotic activity *in vitro* in lung cancer cell lines.

MATERIALS AND METHODS

The active ingredient, febuxostat (FBX), was obtained from (SPIMACO. Al-Qassem, Saudi Arabia) as a gift sample. TPGS and dialysis membrane of 12 kDa cutoff were purchased from Sigma Aldrich, USA. The rest of the chemicals used in this current experiment were of analytical grade. This research project was conducted at the faculty of Pharmacy, King Abdul-Aziz university, Jeddah, Saudi Arabia and Cell Culture Lab, Egyptian Organization for Biological Products and Vaccines (VACSERA Holding Company, Giza, Egypt from April 2019 to Feb 2020. Thereafter, the obtained data were compiled to bring up into this manuscript.

Preparation of FBX loaded TPGS micelles: FBX-loaded TPGS-micelles were formulated by thin-film hydration method[18]. In this process, the micelles were prepared by dissolving FBX (50 mg) and TPGS (500 mg), in ethanol *via* constant stirring using a magnetic stirrer for a duration of 5 min. Distilled water was then added to the prepared solution. Subsequently, ethanol was evaporated from the dispersion by a rotary evaporator (BÜCHI Labortechnik AG, Flawil, Switzerland), which lead to the formation of TPGS thin-film dispersed with FBX. Micelles were formed by hydration of TPGS thin film with water with agitation. The prepared dispersion was then centrifuged at 30,000 rpm for 45 min at 4°C followed by filtration of supernatant using cellulose acetate membrane filter. The residue was lyophilized using a freeze dryer (alpha 1-2 LD plus lyophilizer; Christ, Osterode am Harz, Germany) for 48 hr and stored for further characterization. Miceller formulations were developed with different concentration levels of TPGS (Table 1) to obtain higher drug encapsulation of

Table 1: Formulas of micelle formulations with different concentrations of TPGS and particle size, polydispersity and encapsulation efficiency of TPGS micelles

Formulation	FBX content	TPGS concentration	Particle size ±SD	Polydispersity index ±SD	Encapsulation efficiency ±SD
FBX-TPGS- M1	50 mg	50 mg	163.4±9.5	0.287±0.019	78.46±1.530
FBX-TPGS- M2	50 mg	100 mg	166.2±16.7	0.360±0.032	86.25±0.915
FBX-TPGS- M3	50 mg	150 mg	156.2±11.2	0.255±0.014	93.52±1.120

the micelles and controlled release of drug from the formulated formulations. *Evaluation of FBX-TPGS micelles.*

Mean particle size and polydispersity index (PDI): The prepared FBX-TPGS micelle dispersions were investigated for mean particle size and PDI by dynamic light scattering technique using a Zetasizer Nano ZSP (Malvern Instruments, Worcestershire, UK).

Determination of surface morphology of the micelle: The surface morphology and shape of the formulated FBX-TPGS-M dispersion was examined by transmission electron microscopy (TEM) system (100CX; JEOL, Tokyo, Japan). Before visualization, a sample drop of diluted FBX-TPGS-M was placed onto a microscope grid and dried on the grid after staining with 2% uranyl acid.

Encapsulation efficiency: The encapsulation efficiency of FBX-TPGS micelles were examined using a UV-visible spectrometer (Shimadzu 2600, Tokyo, Japan) at 315 nm. Briefly, micelles dispersion was diluted in methanol and sonicated for 30 min to disassemble the FBX-TPGS-M to release FBX, followed by filtration through 0.22 µm membrane filter to remove undissolved polymeric content. After dilution with an appropriate solvent, the optical absorbance of the sample was determined in a UV spectrophotometer. The encapsulation efficiency of the miceller delivery was calculated as the percentage of the encapsulated FBX among the total amount of FBX, using the standard curve of pure FBX. Following formula[19] was used to determine the encapsulation efficiency of FBX-TPGS micelles:

$$\text{Encapsulation efficiency}(\%) = \frac{\text{Weight of the drug in FBX} - \text{TPGS} - \text{M}}{\text{Weight of the drug}} \times 100$$

***In vitro* drug release of FBX-TPGS-M:** Time-dependent release of FBX from the formulated micelle was evaluated by the dialysis bag method in which FBX-TPGS-M (equivalent to 3 mg of FBX) was placed in a dialysis bag (12 kDa cut off, Sigma Aldrich, USA) and closed from both the ends[20]. This dialysis bag was submerged into phosphate buffer saline (pH 7.4) with stirring at 100 rpm at 37°C. Afterward, 0.5 mL of the sample was withdrawn at a definite time interval, 0.5, 1.0, 2.0, 4.0, 6.0, 8.0, 10.0 and 12.0 hr. and the content of the released drug was measured using a spectrophotometric method at pre-mentioned wavelength.

***In vitro* xanthine oxidase assay:** Determination of xanthine oxidase inhibitory effect was performed in a reaction mixture containing xanthine (2.5-20 µM) and xanthine oxidase (1.1 µg protein equivalent) in phosphate buffer saline (pH 7.4). Addition of the enzyme results in the production of uric acid from xanthine, which was estimated at 292 nm using a UV-visible spectrophotometer. Different concentrations of FBX-TPGS-M, TPGS and FBX were tested to determine the IC50 value of the tested substances[21].

Cell lines and cell culture: Adenocarcinomic human alveolar basal epithelial cells (A549) were obtained from ATCC (King Fahd medical centre, Jeddah, Saudi Arabia) and maintained in mammalian cell culture media (RPMI 1640, Life Technologies (Carlsbad, CA) which was supplemented with 10 U mL^{-1} penicillin and 10 µg mL^{-1} streptomycin, 10% (v/v) fetal bovine serum and 0.25 µg mL^{-1} of amphotericin B in a humidified environment of 37°C, 5% CO_2.

Cytotoxicity assay: Cytotoxicity of FBX-TPGS-M, TPGS and FBX in A549 cell lines was evaluated adopting MTT assay. A549 cells were seeded at the density of 5×103 cells onto each well of 96-well plates and incubate for 24 h. After incubation, the cells were treated with a specific concentration of free FBX, TPGS and FBX-TPGS-M for 24 hr. Subsequently, free drug, TPGS and drug-loaded micelles were removed and treated cells were incubated with MTT solution (0.5%, w/v) for 4 hr. Finally, after the removal of the MTT solution, cells were exposed to 150 µL DMSO for the removal of formazan crystals. The number of living cells was calculated based on the optical density of formazan at 490 nm using ELISA microplate reader (Thermo Fisher Scientific, MA, USA).

Cell cycle analysis: Determination of cell cycle distribution was estimated by the treatment of FBX-TPGS-M, TPGS and free FBX in A549 cell lines for 24 hr following the method depicted by Ling *et al.*[22]. Following this, the cells were harvested and

75% ethanol was used to fix it at 20°C overnight. At that point, the cells were incubated with 5 µg mL^{-1} propidium iodide and 5 µg mL^{-1} of RNase for 3 hr at room temperature in the dark. Subsequently, the number of cells at different stages of the cell cycle was analyzed by using a flow cytometer (FACS Calibur, BD Bioscience, USA). Data of 10,000 cells were composed for each data file, where the obtained data were analyzed by using the Multicycle software (Phoenix Flow Systems, San Diego, CA).

Analysis of apoptosis: Consequently, a double staining technique was used to evaluate the apoptotic effect of FBX-TPGS-M, TPGS and FBX on A549 cell lines. Apoptosis of cells was assessed by an Annexin V-fluorescein isothiocyanate (FITC) conjugate and propidium iodide. Firstly, the A549 cells were exposed to the test materials containing media for a definite period. Subsequently, the cells were washed with phosphate buffer to remove free drug with micelles and processed for assay according to the instruction of apoptosis detection kit (BioVision, CA, USA). Flow cytometer (Epics Profile Analyzer; Coulter Co., Miami, FL) were used to analyze the sample and obtained data were evaluated via Multicycle software (Phoenix Flow Systems, San Diego, CA).

Caspase -3 activity: The cells (5×103 cells) were seeded in a 96-well plate. After 24 hr control, TPGS, FBX and FBX- TPGS micelles were put into the wells to induce apoptosis. Caspase-3 activity was observed as per manufacturer instructions (BioVision, CA, USA).

Statistical analysis: Statistical analysis was performed by Student's t-test between two groups and one-way ANOVA for multiple groups. All results are given as Mean±SD. Differences are considered statistically significant at a level of $p<0.05$.

RESULTS AND DISCUSSION

Particle size and analysis of polydispersity index: The particle size of the formulated micelle along with the polydispersity index of the FBX- TPGS-M was depicted in Table 1. A true reflection of the particle size was measured using the multimodal analysis principle of dynamic light scattering in Zetasizer. Thus, the particle size distribution curves of the samples were found to be unimodal. The mean sizes of the FBX loaded nanomicelles (FBX-TPGS-M1, M2 and M3) were 163.4±9.5, 166.2±16.7 and 156.2±11.2, respectively. The PDI range for the formulated micelles was showed narrow, less than 0.360. Nanocarriers within the size range of 200 nm are known to have enhanced the EPR effect to target more on the cancerous cells due to prolonged circulation, high vasculature of the cancerous area with leaky blood vessels[23,24].

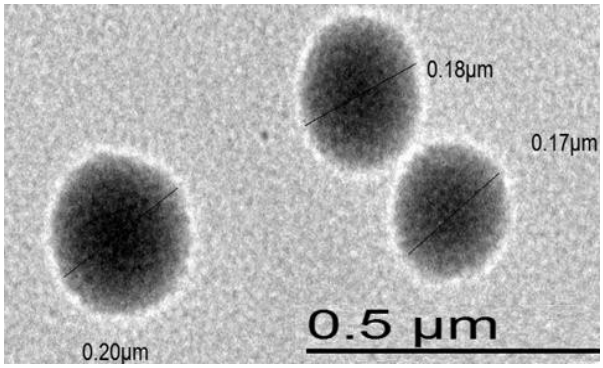

Fig. 1: Transmission electron microscope (TEM) image of the FBX-TPGS-M Encapsulation efficiency of the FBX-TPGS-M

Surface morphology of the FBX-TPGS-M by TEM study: Sizes of the developed nanomicelles were found to be less than 200 nm, thus the scale for the TEM analysis was set to 200 nm to measure the surface morphology. The Uniform shape of the FBX-loaded TPGS micelles revealed a spherical shape in Fig. 1. The sizes obtained by TEM analysis are also in agreement with the photon correlation spectroscopic analysis.

Encapsulation of FBX within the hydrophobic core of the micelles was calculated as a percentage ratio by the provided formula. The encapsulation efficiency of FBX of the TPGS micelles varied as the concentration of TPGS increased in different batches (Table 1). The highest encapsulation efficiency was observed in micelles formulated with the highest concentration of TPGS (150 mg) and it was 93.52±1.120. The observation of increased encapsulation efficiency with an increase in the concentration of TPGS is in line with the findings of Muthu *et al.*[25], where the authors demonstrated an increase in encapsulation efficiency with the amount of TPGS in the nanomicellar formulations. The higher encapsulation of the drug through this experimental design may be explained by the formation of solid dispersion of the drug and TPGS when they were dissolved in ethanol during the manufacturing process of micelles[26]. Considering the observed outcomes on different batches of FBX-TPGS-M concerning particle size, PDI and encapsulation efficiency of FBX, the formulation FBX-TPGS- M3 was found satisfactory for further analysis for release study and cell culture assays.

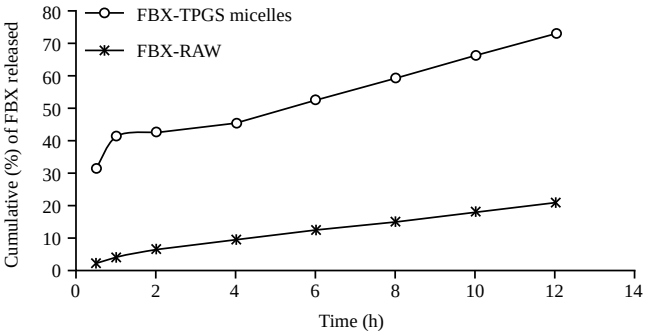

Fig. 2: *In vitro* release profiles of FBX-TPGS-M3 and FBX suspension in phosphate buffer saline (pH 7.4)

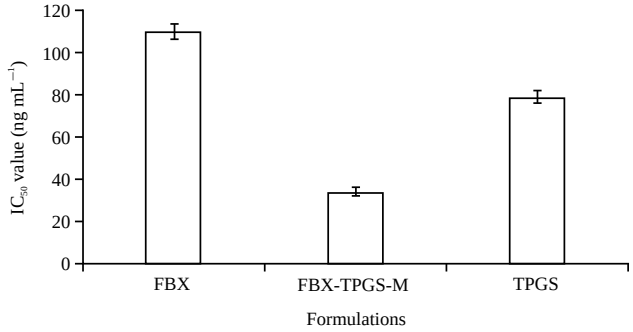

Fig. 3: The IC_{50} values (ng mL^{-1}) of various formulations on xanthine oxidase inhibition. Values are expressed as Mean±SD (n = 3)

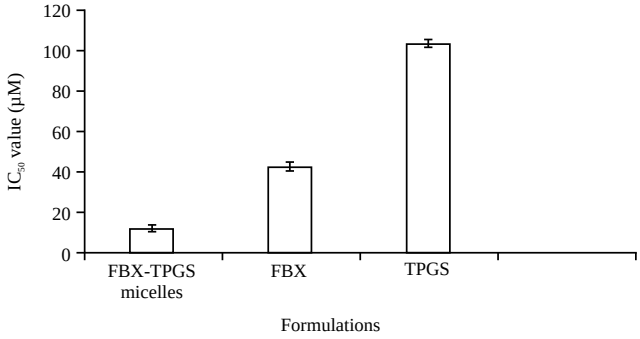

Fig. 4: The IC_{50} values (µM) of FBX-TPGS-micelles, FBX and TPGS treated in A549 cells. The data are presented as Mean±SD (n = 3)

***In vitro* release studies of the FBX loaded TPGS micelles:** *In vitro* release of FBX from FBX-TPGS-M was measured in phosphate buffer saline (pH 7.4) and the percentage release of FBX from the TPGS micelle is displayed in Fig. 2. The release of FBX was found to be 72.7% from FBX-TPGS-M, which was much higher than that of the suspension of the same drug (20.9%). It can be understood that the nano-sized micelles of FBX-TPGS-M preferred transportation through the pores of the dialysis membrane, to release the drug from the micelles. The release of free drugs from the suspension was incomplete, which might be attributed to the fact of the low solubility of the drug. Therefore, our findings revealed the concept of nanocarrier help to improve release characteristics of the poorly water-soluble drugs[20,27].

Xanthine oxidase activity of FBX loaded TPGS micelles: The miceller delivery of FBX exhibited a superior inhibitory in the formation of uric acid by inhibiting xanthine oxidase. Such an inhibitory effect was found to be in a concentration-dependent, where at 10-500 ng mL^{-1} concentration range of FBX through micelllar delivery found to inhibit 11 to 92%, respectively. The IC_{50} value of the FBX-TPGS-M3 was recorded as 33.9±2.17 ng mL^{-1}, whereas the IC50 value of the FBX suspension and TPGS were found to be 109.6±3.62 ng mL^{-1} and 78.87±2.82 ng mL^{-1} (Fig. 3).

Cytotoxicity study: *In vitro* cytotoxicity of components is mainly facilitated by mitochondrial impairment, that indicative probe is determined in MTT assay. To experiment, A549 cells were incubated separately with FBX-TPGS-M, TPGS and free FBX. In this experiment, the IC^{50} value of FBX- TPGS-M was found to be 11.9 µM, whereas the IC^{50} values of TPGS and free FBX were recorded as 42.31 µM and 103.09 µM, respectively (Fig. 4). FBX-TPGS-M depicted a sharp decrease of IC^{50} value, which might be explained by increased intracellular transportation of nanosized micelles into the cancer cells to induce cytotoxicity of the formulation.

Cell cycle analysis: The effect of FBX-TPGS-micelles, FBX and TPGS on various phases of cell cycle was studied in A549 cells through flow cytometry analysis as shown in Fig. 5. The result indicates there was significant increase in cell arrest at G2/M phase when treated with FBX-TPGS-M (23.55±1.16%) compared to free FBX (13.35±1.25%) ($p<0.05$) and control group (9.1±0.71%) ($p<0.01$) (Fig. 5). FBX-TPGS-M (15.29±1.21%) showed a substantial increase in the percentage of cells in pre G1 phase compared to free FBX (3.29±0.24%). Cellular proliferation is imperative in the regulation of the cell cycle, where the cell cycle abnormality is leading to cancer[28]. Cyclins, cyclin-dependent kinases and inhibitors of cyclin-dependent kinases organize G1-phase alteration. Dysregulation of two members, p15 and p21, of inhibitors of cyclin-dependent kinases known to lead cancers[29]. It is interesting to demonstrate that the arrest of the

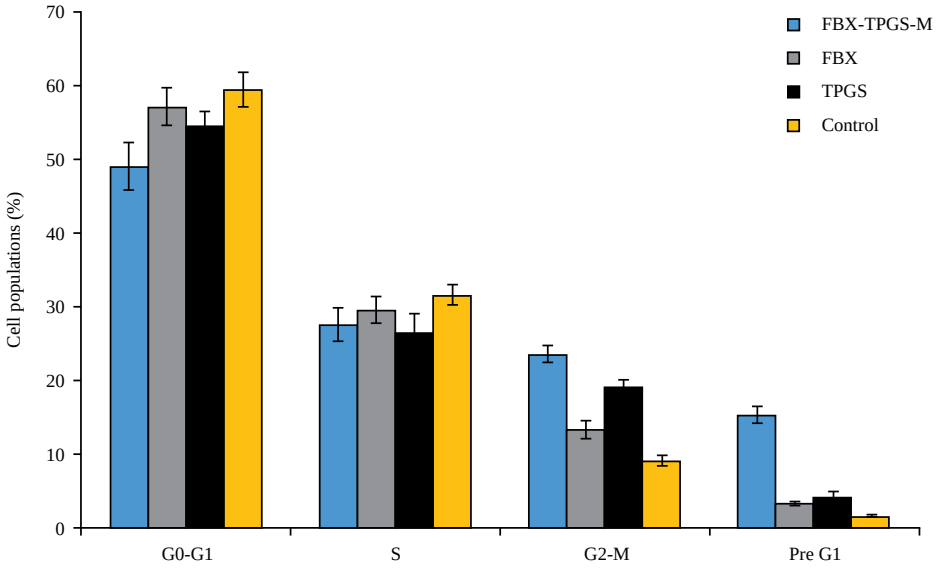

Fig. 5: Cell cycle analysis of A549 cells exposed with IC50 concentration of FBX-TPGS-M, Free FBX, TPGS and control group results are represented as the Mean±SD of 3 distinct findings *p<0.05 (FBX-TPGS-M vs. FBX), **p<0.01 (FBX-TPGS-M vs. control)

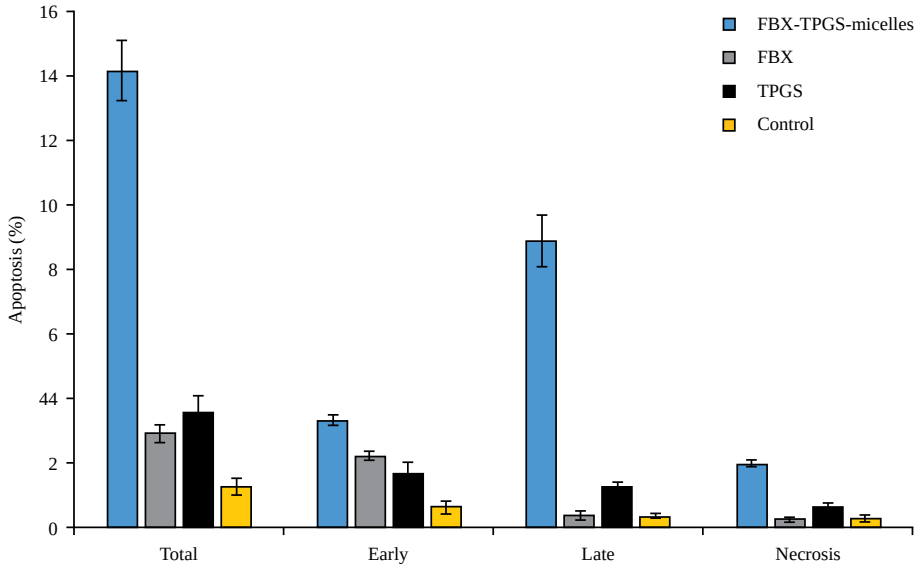

Fig. 6: Apoptosis induction in A549 lung cancer cells treated with Control, TPGS, FBX and FBX-TPGS micelle analyzed using flow cytometry after staining with Annexin V and PI

G2/M phase by TPGS is statistically significant ($p<0.05$), when compared to free FBX. These results are in agreement with some previous reports[30,31]. Thus, it could be assumed that the increased cell arrest in the G2/M phase of cell proliferation by FBX-TPGS-M might be due to the synergistic effect of miceller delivery to increase the cellular concentration of the drug and presence of TPGS. This is the first evidence to represent that FBX inhibits cell proliferation through the downregulation of p15 and p21 genes[19].

Determination of apoptotic potential and Caspase 3: Annexin-PI staining method was performed to determine the proportion of apoptotic and death cells by treating with control group, TPGS, FBX and FBX-TPGS micelles as shown in Fig. 6. The FBX-TPGS micelles (14.22±0.92%) showed substantial increased in the percentage of apoptotic cells as compared to FBX (2.93±0.28%), TPGS (3.63±0.47%) and control group (1.29±0.25%). Alfaifi *et al.*[31] showed in previous reports that polyethylene coated PLGA nanoparticles of FBX

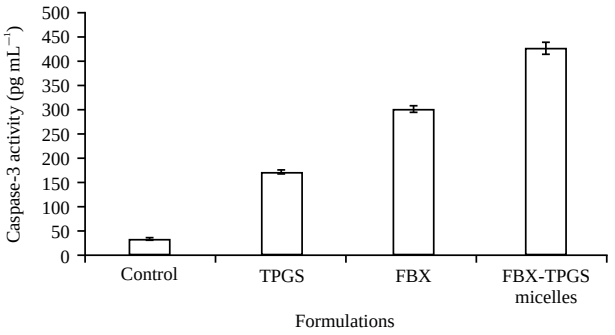

Fig. 7: Effects of different formulations on caspase-3 activity in A549 cells

considerably inhibited cell proliferation in A549 cells as compared to FBX. Further, caspase-3 activation and loss in cell membrane integrity are interlinked during cellular apoptosis[32]. Here, we have observed that the significant increase in caspase-3 production (426±13 pg mL^{-1}, $p<0.01$) during incubation of A549 cells with FBX-TPGS micelles, when compared with free FBX treated groups (300.6±6.81 pg mL^{-1}) (Fig. 7).

CONCLUSION

In summary, the method employed in this current experiment for formulating FBX micelle was able to entrap a sufficient quantity of drugs within the nano-sized spherical miceller structure. *In vitro* release profile showed a controlled and higher release of the drug from the TPGS micelles as compared to free FBX. Cytotoxicity study revealed higher cytotoxicity of FBX loaded TPGS micelles than a free FBX with a reduction of 2.5-fold in IC_{50} value in A549 lung cancer cells. Further, cell cycle arrest at G2/M phase, increased percentage of apoptotic cell death and caspase-3 activity by the FBX-TPGS-M as compared to FBX could be due to the downregulation of p15 and p21 genes within the cancer cell. Our findings demonstrate that FBX loaded TPGS micelles could be a potential drug delivery system to improve its anticancer effect for lung cancer therapy.

ACKNOWLEDGMENT

The authors extend their appreciation to the Deanship of Scientific Research at King Khalid University for funding this work through the Research Group project under grant number (R.G.P.1/149/40).

SIGNIFICANCE STATEMENT

TPGS used as a surfactant has a cytotoxicity activity that can be used to formulate micelles loaded with Ellagic acid, which has anticancer activity. This combination improved febuxostat as a repurposed drug for anticancer activity. Our data confirm these findings and open the way for further work of using eco- friendly surfactants.

REFERENCES

1. Gorain, B., H. Choudhury, M. Pandey, A.B. Nair and M.C.I.M. Amin *et al*., 2019. Dendrimer-based Nanocarriers in Lung Cancer Therapy. In: Nanotechnology-based Targeted Drug Delivery Systems for Lung Cancer, Kesharwani, P. (Ed.). Chapter 7, Academic Press, New York, USA., ISBN: 978-0-12-815720-6, pp: 161-192.
2. Cheng, W., C. Liang, L. Xu, G. Liu and N. Gao *et al*., 2017. TPGS-functionalized polydopamine-modified mesoporous silica as drug nanocarriers for enhanced lung cancer chemotherapy against multidrug resistance. Small, 10.1002/smll.201700623
3. Butler, K.S., P.N. Durfee, C. Theron, C.E. Ashley, E.C. Carnes and C.J. Brinker, 2016. Protocells: modular mesoporous silica nanoparticle-supported lipid bilayers for drug delivery. Small, 12: 2173-2185.
4. Choudhury, H., M. Pandey, T.H. Yin, T. Kaur and G.W. Jia *et al*., 2019. Rising horizon in circumventing multidrug resistance in chemotherapy with nanotechnology. Mater. Sci. Eng.: C, 101: 596-613.
5. Choudhury, H., B. Gorain, M. Pandey, S.A. Kumbhar, R.K. Tekade, A.K. Iyer and P. Kesharwani, 2017. Recent advances in TPGS-based nanoparticles of docetaxel for improved chemotherapy. Int. J. Pharm., 529: 506-522.
6. Sonali, P. Agrawal, R.P. Singh, C.V. Rajesh and S. Singh *et al*., 2016. Transferrin receptor-targeted vitamin E TPGS micelles for brain cancer therapy: preparation, characterization and brain distribution in rats. Drug Delivery, 23: 1788-1798.
7. Brinkman, A.M., G. Chen, Y. Wang, C.J. Hedman and N.M. Sherer *et al*., 2016. Aminoflavone-loaded EGFR-targeted unimolecular micelle nanoparticles exhibit anti-cancer effects in triple negative breast cancer. Biomater., 101: 20-31.
8. Movassaghian, S., O.M. Merkel and V.P. Torchilin, 2015. Applications of polymer micelles for imaging and drug delivery. Wiley Interdiscip. Rev.: Nanomed. Nanobiotechnol., 7: 691-707.
9. Bernabeu, E., L. Gonzalez, M. Cagel, E.P. Gergic and M.A. Moretton *et al*., 2016. Novel Soluplus®-TPGS mixed micelles for encapsulation of paclitaxel with enhanced *in vitro* cytotoxicity on breast and ovarian cancer cell lines. Colloids Surf. B. Biointerfaces, 140: 403-411.

10. Wang, Y., Y. Ding, J. Zhao, C. Wang and M. Gao *et al*., 2019. Dihydroartemisinin and doxorubicin co-loaded Soluplus®-TPGS mixed micelles: Formulation characterization, cellular uptake and pharmacodynamic studies. Pharm. Dev. Technol., 24: 1125-1132.
11. Mi, Y., Y. Liu and S.S. Feng, 2011. Formulation of Docetaxel by folic acid-conjugated d-a-tocopheryl polyethylene glycol succinate 2000 (Vitamin E TPGS2k) micelles for targeted and synergistic chemotherapy. Biomater., 32: 4058-4066.
12. Liu, G., H.I. Tsai, X. Zeng, W. Cheng and L. Jiang *et al*., 2018. Phosphorylcholine-based stealthy nanocapsules decorating TPGS for combatting multi-drug-resistant cancer. ACS Biomater. Sci. Eng., 4: 1679-1686.
13. Sun, M., X. Wang, X. Cheng, L. He, G. Yan and R. Tang, 2018. TPGS-functionalized and ortho ester-crosslinked dextran nanogels for enhanced cytotoxicity on multidrug resistant tumor cells. Carbohydr. Polym., 198: 142-154.
14. Perez-Ruiz, A.G., A. Ganem, I.M. Olivares-Corichi and J.R. García-Sánchez, 2018. Lecithin–chitosan–TPGS nanoparticles as nanocarriers of (−)-epicatechin enhanced its anticancer activity in breast cancer cells. RSC Adv., 8: 34773-34782.
15. Feng, S.S., 2006. New-concept chemotherapy by nanoparticles of biodegradable polymers: Where are we now? Nanomed., 1: 297-309.
16. Choudhury, H., B. Gorain, A. Das, B. Ghosh and T. Pal, 2014. Development and validation of a sensitive HPLC-MS/MS-ESI method for determination of febuxostat: application to pharmacokinetic study. Curr. Anal. Chem., 10: 528-536.
17. Tamura, K., Y. Kawai, T. Kiguchi, M. Okamoto and M. Kaneko *et al*., 2016. Efficacy and safety of febuxostat for prevention of tumor lysis syndrome in patients with malignant tumors receiving chemotherapy: a phase III, randomized, multi-center trial comparing febuxostat and allopurinol. Int. J. Clin. Oncol., 21: 996-1003.
18. Ai, X., L. Zhong, H. Niu and Z. He, 2014. Thin-film hydration preparation method and stability test of DOX-loaded disulfide-linked polyethylene glycol 5000-lysine-di-tocopherol succinate nanomicelles. Asian J. Pharm. Sci., 9: 244-250.
19. Shadab , M.Y. Alfaifi, S.E.I. Elbehairi, A.A. Shati, U.A. Fahmy and N.A. Alhakamy, 2020. Ellagic acid loaded TPGS micelles for enhanced anticancer activities in ovarian cancer. Int. J. Pharmacol., 16: 63-71.
20. Choudhury, H., B. Gorain, S. Karmakar, E. Biswas and G. Dey *et al*., 2014. Improvement of cellular uptake, *in vitro* antitumor activity and sustained release profile with increased bioavailability from a nanoemulsion platform. Int. J. Pharm., 460: 131-143.
21. Takano, Y., K. Hase-Aoki, H. Horiuchi, L. Zhao, Y. Kasahara, S. Kondo and M.A. Becker, 2005. Selectivity of febuxostat, a novel non-purine inhibitor of xanthine oxidase/xanthine dehydrogenase. Life Sci., 76: 1835-1847.
22. Ling, Y.H., L. Liebes, J.D. Jiang, J.F. Holland and P.J. Elliott *et al*., 2003. Mechanisms of proteasome inhibitor PS-341-induced G_2-M-phase arrest and apoptosis in human non-small cell lung cancer cell lines. Clin. Cancer Res., 9: 1145-1154.
23. Choudhury, H., B. Gorain, M. Pandey, R. Kaur and P. Kesharwani, 2019. Strategizing biodegradable polymeric nanoparticles to cross the biological barriers for cancer targeting. Int. J. Pharm., 565: 509-522.
24. Muthu, M.S., R.V. Kutty, Z. Luo, J. Xie and S.S. Feng, 2015. Theranostic vitamin E TPGS micelles of transferrin conjugation for targeted co-delivery of docetaxel and ultra bright gold nanoclusters. Biomater., 39: 234-248.
25. Muthu, M.S., S.A. Kulkarni, Y. Liu and S.S. Feng, 2012. Development of docetaxel-loaded vitamin E TPGS micelles: formulation optimization, effects on brain cancer cells and biodistribution in rats. Nanomed., 7: 353-364.
26. Tyrrell, Z.L., Y. Shen and M. Radosz, 2010. Fabrication of micellar nanoparticles for drug delivery through the self-assembly of block copolymers. Progr. Polym. Sci., 35: 1128-1143.
27. Gao, F., Z. Zhang, H. Bu, Y. Huang and Z. Gao *et al*., 2011. Nanoemulsion improves the oral absorption of candesartan cilexetil in rats: Performance and mechanism. J. Control. Release, 149: 168-174.
28. Massagué, J., 2004. G1 cell-cycle control and cancer. Nature, 432: 298-306.
29. Chen, W., M. Huang, D. Sun, R. Kong and T. Xu *et al*., 2016. Long intergenic non-coding RNA 00152 promotes tumor cell cycle progression by binding to EZH2 and repressing p15 and p21 in gastric cancer. Oncotarget, 7: 9773-9787.
30. Alhakamy, N.A. and Shadab, 2019. Repurposing itraconazole loaded PLGA nanoparticles for improved antitumor efficacy in non-small cell lung cancers. Pharm., 10.3390/pharmaceutics11120685
31. Alfaifi, M.Y., A.A. Shati, S.E.I. Elbehairi, U.A. Fahmy, N.A. Alhakamy and Shadab, 2020. Anti-tumor effect of PEG-coated PLGA nanoparticles of febuxostat on A549 non-small cell lung cancer cells. 3 Biotech., 10.1007/s13205-020-2077-x
32. Moghimi, S.M., P. Symonds, J.C. Murray, A.C. Hunter, G. Debska and A. Szewczyk, 2005. A two-stage poly (ethylenimine)-mediated cytotoxicity: Implications for gene transfer/therapy. Mol. Ther., 11: 990-995.